IAI Journals.ASM.org

Macrophage-Inducible C-Type Lectin Mincle-Expressing Dendritic Cells Contribute to Control of Splenic *Mycobacterium bovis* BCG Infection in Mice

Friederike Behler,[a] Regina Maus,[a] Jennifer Bohling,[a] Sarah Knippenberg,[a] Gabriele Kirchhof,[a] Masahiro Nagata,[d] Danny Jonigk,[b] Nicole Izykowski,[b] Lavinia Mägel,[b] Tobias Welte,[c,e] Sho Yamasaki,[d] Ulrich A. Maus[a,e]

Department of Experimental Pneumology,[a] Institute of Pathology,[b] and Clinic for Pneumology,[c] Hannover Medical School, Hannover, Germany; Division of Molecular Immunology, Medical Institute of Bioregulation, Kyushu University, Fukuoka, Japan[d]; German Center for Infectious Diseases DZIF, Hannover, Germany[e]

The macrophage-inducible C-type lectin Mincle has recently been identified to be a pattern recognition receptor sensing mycobacterial infection via recognition of the mycobacterial cell wall component trehalose-6′,6-dimycolate (TDM). However, its role in systemic mycobacterial infections has not been examined so far. Mincle-knockout (KO) mice were infected intravenously with *Mycobacterium bovis* BCG to mimic the systemic spread of mycobacteria under defined experimental conditions. After intravenous infection with *M. bovis* BCG, Mincle-KO mice responded with significantly higher numbers of mycobacterial CFU in spleen and liver, while reduced granuloma formation was observed only in the spleen. At the same time, reduced Th1 cytokine production and decreased numbers of gamma interferon-producing T cells were observed in the spleens of Mincle-KO mice relative to the numbers in the spleens of wild-type (WT) mice. The effect of adoptive transfer of defined WT leukocyte subsets generated from bone marrow cells of zDC$^{+/DTR}$ mice (which bear the human diphtheria toxin receptor [DTR] under the control of the classical dendritic cell-specific zinc finger transcription factor zDC) to specifically deplete Mincle-expressing classical dendritic cells (cDCs) but not macrophages after diphtheria toxin application on the numbers of splenic and hepatic CFU and T cell subsets was then determined. Adoptive transfer experiments revealed that Mincle-expressing splenic cDCs rather than Mincle-expressing macrophages contributed to the reconstitution of attenuated splenic antimycobacterial immune responses in Mincle-KO mice after intravenous challenge with BCG. Collectively, we show that expression of Mincle, particularly by cDCs, contributes to the control of splenic *M. bovis* BCG infection in mice.

Mycobacterium tuberculosis is the causative pathogen of pulmonary tuberculosis (TB) and is the second leading cause of infection-induced death worldwide. One-third of the world's population is considered to be infected with *M. tuberculosis* and approximately 8.7 million newly emerging TB cases and 1.4 million deaths annually have been reported by the World Health Organization, with *M. tuberculosis* thereby representing a global health threat (1). Inhalation of *M. tuberculosis*-containing aerosols establishes pulmonary infections with *M. tuberculosis*, where lung professional phagocytes, such as resident alveolar macrophages, are the primary cellular niche for this pathogen (2, 3).

A hallmark of the lung antimycobacterial defense against local mycobacterial spread and dissemination is the formation of a granuloma (4–7), which typically consists of inflammatory mononuclear cell aggregates, mainly foamy macrophages surrounded by lymphocyte subsets. Within such granulomas, mycobacteria can persist in a dormant state, termed latency (4, 8–10). Under certain conditions, dormant mycobacteria are reactivated and frequently disseminate to extrapulmonary organ systems, thereby establishing a severe clinical complication of pulmonary tuberculosis (8, 11–13). Notably, not only *M. tuberculosis* but also *M. bovis* BCG may cause mycobacterial dissemination in humans, as has been noted, e.g., in patients treated by intravesical *M. bovis* BCG therapy for bladder cancer, which may lead to systemic BCGitis, a severe systemic BCG infection (14). Therefore, elucidation of the molecular pathways underlying the control of systemic *M. bovis* BCG infection may also inform about the regulatory pathways controlling *M. tuberculosis* dissemination.

The macrophage-inducible C-type lectin Mincle (also called Clec4e or Clecsf9) is a transcriptional target of NF–interleukin-6 (IL-6) (C/EBPβ) and is expressed on professional antigen-presenting cells (APCs), such as macrophages, dendritic cells (DCs), B cells, and neutrophils, in response to several inflammatory stimuli (15, 16). Mincle is a type II transmembrane protein and an activating receptor coupled to the FcRγ chain, an immunoreceptor tyrosine-based activation motif (ITAM)-containing adaptor, and recognizes the mycobacterial cell wall component trehalose-6′,6-dimycolate (TDM; cord factor) of *M. tuberculosis* as well as its synthetic analogue, trehalose-dibehenate (TDB) (17–19). Activation of Mincle is further induced in response to endogenous danger signals, such as SAP130, a small ribonucleoprotein released by dying cells (17), or is induced in response to pathogenic fungi

Received 15 August 2014 **Returned for modification** 8 September 2014
Accepted 13 October 2014

Accepted manuscript posted online 20 October 2014

Citation Behler F, Maus R, Bohling J, Knippenberg S, Kirchhof G, Nagata M, Jonigk D, Izykowski N, Mägel L, Welte T, Yamasaki S, Maus UA. 2015. Macrophage-inducible C-type lectin Mincle-expressing dendritic cells contribute to control of splenic *Mycobacterium bovis* BCG infection in mice. Infect Immun 83:184–196. doi:10.1128/IAI.02500-14.

Editor: S. Ehrt

Address correspondence to Ulrich A. Maus, Maus.Ulrich@mh-hannover.de.

Supplemental material for this article may be found at http://dx.doi.org/10.1128/IAI.02500-14.

doi:10.1128/IAI.02500-14

(20–22). Downstream receptor activation involves the Syk-CARD9-BCL10-Malt1 signaling pathway and results in a Th1 and Th17 cytokine-dominated immune response (19, 23).

Our group recently showed that Mincle is expressed as a delayed-type pattern recognition receptor on alveolar macrophages, newly recruited exudate macrophages, and alveolar recruited neutrophils in response to *M. bovis* BCG infection, where it critically shapes the lung inflammatory response against mycobacterial challenge (24). In that study, we observed that Mincle-knockout (KO) mice were more susceptible to intravenous *M. bovis* BCG infection, suggesting that Mincle might play a role in the regulation of systemic mycobacterial infection. Capitalizing on these findings, we examined here the role of Mincle in the splenic and hepatic response to intravenous BCG infection in wild-type (WT) and Mincle-KO mice.

MATERIALS AND METHODS

Animals. WT C57BL/6 mice were purchased from Charles River (Sulzfeld, Germany). Mincle-KO mice on a C57BL/6 background (21) were obtained from the Consortium for Functional Glycomics (CFG). CD45.1 alloantigen-expressing C57BL/6 mice (B6.SJL-Ptprca) were purchased from The Jackson Laboratory (Sacramento, CA). Transgenic zDC$^{+/DTR}$ mice on a C57BL/6 background bearing the human diphtheria toxin receptor (DTR) under the control of the classical dendritic cell-specific zinc finger transcription factor zDC (also termed Zbtb46 and Btbd4) were generously provided by Michel Nussenzweig (The Rockefeller University, New York, NY) (25). Animals were used at 8 to 12 weeks of age according to the guidelines of the Institutional Animal Care and Use Committee of Hannover Medical School. Animal experiments were approved by the Lower Saxony State Office for Consumer Protection and Food Safety (Hannover, Germany).

Reagents. Rat monoclonal anti-Mincle antibody (Ab; clone 1B6, IgG1κ) was generated as recently described (17), and the respective purified rat IgG1κ isotype control (clone R3-34) was purchased from BD Biosciences (Heidelberg, Germany). Anti-CD3 fluorescein isothiocyanate (FITC; clone 145-2C11), anti-CD4-peridinin chlorophyll protein-Cy5.5 (clone RM4-5), anti-CD8-phycoerythrin (PE)-Cy7 (clone 53-6.7), anti-CD11b-PE-Cy7 (clone M1/70), anti-CD19-PE (clone 1D3), anti-CD45.1-FITC (clone A20), anti-CD45.2-PE (clone 30F11), anti-gamma interferon (anti-IFN-γ)-allophycocyanin (APC) (clone XMG1.2), anti-Ly6G-PE (clone 1A8), biotinylated IgG1 (clone RG11/39.4), and allophycocyanin-streptavidin were all obtained from BD Biosciences (Heidelberg, Germany). Anti-F4/80-FITC (clone CI:A3-1) and anti-F4/80-APC (clone CI:A3-1) were obtained from Serotec (Düsseldorf, Germany). Anti-CD11c-PE-Cy5.5 (clone N418) was purchased from Invitrogen, and anti-major histocompatibility complex class II (anti-MHC-II) eFluor 450 (clone M5/114.15.2) was obtained from eBioscience (San Diego, CA, USA). A magnetically activated cell sorting (MACS) kit and CD19 and CD90.2 Ab-labeled magnetic beads for purification of splenic T and B cells as well as CD45 Ab-labeled magnetic beads for purification of hepatic leukocytes were obtained from Miltenyi Biotec (Bergisch Gladbach, Germany). Diphtheria toxin (DT) was purchased from Sigma (Deisenhofen, Germany).

Analysis of TDM from *M. bovis* as a specific ligand for Mincle. To verify that TDM from *M. bovis* (and *M. bovis* BCG derived therefrom) is recognized by Mincle, green fluorescent protein (GFP)-conjugated NFAT (NFAT-GFP) reporter cells expressing either Mincle plus FcRγ or FcRγ only were cultured in RPMI 1640 medium enriched with 10% fetal calf serum (FCS) and β-mercaptoethanol, followed by stimulation with different concentrations of plate-coated TDM purified from *M. bovis* (Sigma, Deisenhofen, Germany) for 18 h. Subsequently, reporter cells were subjected to GFP expression analysis by flow cytometry, as described previously (17, 18).

Spleen and liver histopathology and detection of mycobacteria with fluorescence microscopy and ZN staining. Spleens as well as the right and left medial lobes of the liver of *M. bovis* BCG-infected WT and Mincle-KO mice were fixed in 4.5% neutral buffered formalin (Histofix; Roth, Karlsruhe, Germany) for 24 h at room temperature. Paraffin-embedded spleen and liver tissue was sectioned at 3 μm. Histological quantification of splenic macrophages was performed by immunohistochemistry using anti-CD68 Ab (Abcam, Cambridge, United Kingdom). The splenic and hepatic granulomas in 10 and 20 high-power fields (HPFs) were enumerated by an experienced pathologist (D.J.) using an Olympus fluorescence microscope (BX 51TF; Olympus, Hamburg, Germany). For detection of splenic mycobacteria via fluorescence microscopy, formalin-fixed and paraffin-embedded tissue sections were deparaffinized, rehydrated, and then stained with a TB-fluor, phenol-free solution from a staining kit from Merck (Darmstadt, Germany) which consisted of auramine-rhodamine solution, decolorization solution, and counterstaining solution. The slides were processed following the manufacturer's protocol. Sections of spleens were also subjected to Ziehl-Neelsen (ZN) stainings. Briefly, after deparaffinization, slides were stained for 20 min with Ziehl-Neelsen carbol fuchsin solution (Merck, Darmstadt, Germany), which was preheated to 60°C. Following decolorization with HCl-ethanol, the slides were washed with tap water for 10 min and then counterstained with hemalum (Merck).

Culture and quantification of *M. bovis* BCG. *M. bovis* BCG (strain Pasteur) was cultured in Middlebrook 7H9 medium enriched with oleic acid-albumin-dextrose-catalase supplement (BD Biosciences, Heidelberg, Germany) until mid-log phase and then frozen in 1-ml aliquots at −80°C until use. For quantification of the CFU, mycobacteria were serially diluted in Middlebrook 7H9 medium and plated on Middlebrook 7H10 agar plates (BD Biosciences, Heidelberg, Germany). After 3 weeks of incubation at 37°C, the CFU were quantified.

Treatment groups and infection of mice with *M. bovis* BCG. To evaluate the role of Mincle-expressing macrophages versus that of classical dendritic cells (cDCs) on splenic and hepatic antimycobacterial immunity, in selected experiments, each Mincle-KO mouse received via intravenous (i.v.) adoptive transfer 5×10^6 bone marrow-derived monocytes (BMMs) from WT mice, transgenic zDC$^{+/DTR}$ mice, or Mincle-KO mice (as a transfusion control) immediately subsequent to i.v. infection of the mice with *M. bovis* BCG. This was followed by analysis of the mycobacterial loads and the numbers of IFN-γ-producing CD4$^+$ and CD8$^+$ T cells in the spleens and livers (right and left medial lobes) of the mice on days 14 and 21 postinfection. Alternatively, Mincle-KO mice received repetitive adoptive transfer of neutrophils that were purified from the bone marrow of WT or Mincle-KO mice on days 0, 1, and 3 after i.v. *M. bovis* BCG challenge, followed by analysis of the mycobacterial loads and IFN-γ-producing CD4$^+$ and CD8$^+$ T cells in the spleens of the mice on day 7 postinfection.

Adoptive leukocyte transfer and DT-dependent depletion of cDCs. Bone marrow cells were isolated from the tibias and femurs of Mincle-KO mice or CD45.2 alloantigen-expressing transgenic zDC$^{+/DTR}$ mice as described previously (26–28). Briefly, the tibias and femurs were flushed with sterile RPMI 1640 medium supplemented with 10% FCS, and the cells were filtered through a 40-μm-mesh-size cell strainer (BD Biosciences, Heidelberg, Germany) to remove cell aggregates. Subsequently, the cell suspensions were centrifuged at 1,200 rpm for 10 min at 4°C. Thereafter, bone marrow cells were incubated overnight in cell culture dishes (Greiner, Frickenhausen, Germany) in Dulbecco modified Eagle medium (PAA, Pasching, Austria) supplemented with 10% FCS, 2 mM glutamine, 1% penicillin-streptomycin, 1% HEPES (Gibco, Invitrogen, Karlsruhe, Germany), and 1% sodium pyruvate (PAA, Pasching, Austria) at 37°C in 5% CO_2. After 24 h, nonadherent cells were collected and stimulated with 50 ng/ml macrophage colony-stimulating factor (R&D Systems, Wiesbaden, Germany) in cell culture dishes (Sarstedt, Nümbrecht, Germany) for 3 days to enrich monocytic cells. The purities of these cell preparations were always >95%, as determined by fluorescence-activated cell sorter (FACS) analysis of their F4/80 cell surface expression. Such bone marrow-derived monocyte preparations from Mincle-KO mice or zDC$^{+/DTR}$ mice were then intravenously transfused into Mincle-KO mice (5×10^6 cells/

mouse) to study the contribution of Mincle-expressing monocyte-derived DCs, as opposed to monocyte-derived macrophages, to antimycobacterial immunity in BCG-infected recipient Mincle-KO mice.

To ensure the specific depletion of cDCs while sparing macrophages in this experimental setting, we first established a DT-based cDC depletion protocol, based on recent reports (25). Briefly, CD45.1 alloantigen-expressing ($CD45.1^+$) recipient WT mice were i.v. infected with *M. bovis* BCG at 8×10^5 CFU/mouse, and then the mice received a single intravenous transfusion of bone marrow-derived monocytic cells from CD45.2 alloantigen-expressing ($CD45.2^+$) donor $zDC^{+/DTR}$ mice (5×10^6 cells/mouse). Specific depletion of $CD45.2^+$ cDCs but not $CD45.2^+$ macrophages in the spleens of $CD45.1^+$ recipient mice was achieved by intraperitoneal (i.p.) injection of DT (10 ng/g body weight [bw] DT dissolved in phosphate-buffered saline [PBS]) at day 1 and every 48 h for 7 days, followed by FACS analysis of the respective $CD45.2^+$ donor cell populations in the spleens of recipient mice on day 7 postinfection. This protocol was then employed to specifically deplete Mincle-expressing $zDC^{+/DTR}$ cDCs but not macrophages in recipient Mincle-KO mice subsequent to their infection with *M. bovis* BCG on days 14 and 21 postinfection.

For purification of bone marrow-derived neutrophils, bone marrow cells from WT and Mincle-KO mice were isolated as described above and then loaded onto a three-layer Percoll gradient consisting of 2 ml 81%, 2 ml 67%, and 2 ml 52% Percoll Plus (GE Healthcare, Uppsala, Sweden), according to the manufacturer's instructions. After centrifugation at $500 \times g$ for 35 min at 4°C, neutrophils were carefully aspirated from the 81% to 67% interphase and washed with Hanks balanced salt solution (HBSS) supplemented with EDTA and bovine serum albumin (29). The purities of the bone marrow-derived neutrophils used for the transfusion experiments always ranged from 80 to 90%, as judged by FACS analysis of their Ly6G cell surface staining.

Treatment of mice with function-blocking anti-Mincle antibody. In selected experiments, WT mice were intravenously infected with *M. bovis* BCG (8×10^5 CFU/mouse), and then the mice received daily i.p. injections of either function-blocking anti-Mincle antibody 1B6 (10 μg/mouse in 150 μl PBS–0.1% human serum albumin [HSA]) or control IgG1 for 7 or 14 consecutive days, followed by determination of the mycobacterial loads in the spleen on days 14 and 21 postinfection.

Determination of mycobacterial loads in the spleen and liver. Mice were euthanized with an overdose of isoflurane, and the spleens and livers (left lateral lobe, right lateral lobe, and caudate lobe) were isolated and homogenized using a tissue homogenizer (IKA, Staufen, Germany). The resulting spleen and hepatic homogenates were lysed in HBSS containing 0.1% saponin, and 10-fold serial dilutions of homogenates were processed for determination of the number of CFU on 7H10 agar plates (7, 24).

Immunophenotypic analysis of splenic and hepatic leukocyte subsets. The spleens of WT and Mincle-KO mice were isolated and dissected with a sterile scalpel. After crushing of the tissue using a pestle, cells were aspirated with a 1-ml pipette, placed into RPMI 1640 medium, and filtered through a 40-μm-mesh-size cell strainer (BD Biosciences) to obtain single-cell suspensions. Subsequently, splenic T and B cells were enriched using a CD19 and CD90.2 MACS purification kit following the manufacturer's instructions (Miltenyi, Bergisch Gladbach, Germany). Briefly, splenocytes were centrifuged at 1,200 rpm for 10 min at 4°C, and ammonium chloride buffer was added for lysis of red blood cells for 5 min. Thereafter, cells were washed and resuspended in MACS buffer, followed by incubation of the cells with 10 μl each of anti-CD19 and anti-CD90.2 antibody-conjugated magnetic beads per 10^7 cells. Following incubation for 15 min at 4°C, the cells were washed and passed over a MACS LS column to separate $CD19^+$ B cells and $CD90.2^+$ T cells. The liver was perfused with 30 ml HBSS until hepatic vessels were free of blood. The left and right medial lobes of the liver were removed carefully and were then cut into small pieces and incubated in digestion solution (RPMI 1640 medium supplemented with collagenase A [5 mg/ml] and DNase I [1 mg/ml] from Roche, IN) for 30 min. The digested tissue was then filtered through a 70-μm-mesh-size cell strainer and then a 40-μm-mesh-size cell strainer (BD Biosciences). Hepatocytes were centrifuged at 1,000 rpm for 10 min at room temperature (22°C), and the cell pellet was then resuspended in MACS buffer, followed by centrifugation at 800 rpm for 10 min at room temperature. Then, hepatocytes were incubated with 10 μl of anti-CD45 antibody-conjugated magnetic beads per 10^7 cells for 15 min at 4°C. Subsequently, the cells were washed and passed over a MACS LS column to enrich $CD45^+$ hepatic leukocytes. For flow cytometric analysis of splenic and hepatic lymphocyte subsets, cells were incubated with highly purified IgG derived from human plasma (Octagam; Octapharm, Langenfeld, Germany) and were then stained for 20 min at 4°C with appropriately diluted antibodies according to their cell surface antigen expression profiles. For analysis of intracellular IFN-γ expression by the respective T cell subsets, cells were washed twice with FACS buffer and were then incubated with Fix/Perm solution for 20 min at 4°C and washed with Perm/Wash buffer, followed by incubation of the cells with appropriately diluted antibodies for 30 min at 4°C. The cells were then washed twice and resuspended in FACS buffer for flow cytometric analysis. Immunophenotypic analysis of lymphocyte subsets was done by gating according to their forward scatter area (FSC-A) versus side scatter (SSC-A) as well as FSC-A versus forward scatter height (FSC-H) characteristics to exclude cell aggregates, followed by analysis of $CD4^+$ T cells ($CD3^+$ $CD4^+$ $CD8^-$), $CD8^+$ T cells ($CD3^+$ $CD4^-$ $CD8^+$), and B cells ($CD3^-$ $CD19^+$). As a positive control for detection of intracellular IFN-γ, MiCK mouse cytokine-positive control cells (BD Biosciences) were used.

Flow cytometric analysis of splenic myeloid cells within the $CD19^-$ $CD90^-$ leukocyte fraction was done according to previous protocols (30). Gating of the cells was done according to their FSC-A/SSC-A characteristics, while taking care to exclude $FSC\text{-}A^{low}$ and $SSC\text{-}A^{high}$ eosinophils, and by subgating according to their FSC-A/FSC-H characteristics to exclude cell aggregates. Neutrophils were identified as Ly6G-positive ($Ly6G^+$), $SSC\text{-}A^{low}$, and $CD11b^+$ cells. Splenic macrophages were identified as Ly6G-negative ($Ly6G^-$), $SSC\text{-}A^{low}$, $CD11b^{high}$, $CD11c^{low}$, and MHC-II-negative ($MHC\text{-}II^-$)/$MHC\text{-}II^{low}$ cells. Splenic cDCs were identified as $Ly6G^-$, $SSC\text{-}A^{low}$, $CD11b^{mid}$, $CD11c^{high}$, and $MHC\text{-}II^{high}$ cells.

Flow sorting of splenic macrophages, neutrophils, and dendritic cells. Mincle-expressing macrophages and neutrophils are directly involved as antimycobacterial innate effector cells in mycobacterial uptake and killing (7, 24). We performed high-speed cell sorting of Mincle-expressing splenic macrophages and neutrophils as well as dendritic cells for subsequent gene expression analysis using a FACSAria II flow cytometer (BD Biosciences) equipped with a 3-laser system (blue laser, 488-nm excitation wavelength; violet laser, 405-nm wavelength; red laser, 633-nm wavelength). Splenic macrophages, neutrophils, and cDCs were gated as outlined above, and after appropriate compensation setting, cells were sorted with an 85-μm nozzle at a flow rate of ~10,000 particles per second. The complete sorting process was performed at a constant temperature of 4°C, and resort analysis of sorted cells revealed sort purities of >98% (24, 26, 31).

Real-time RT-PCR. Total cellular RNA was isolated from flow-sorted splenic macrophages, neutrophils, and cDCs of mock-infected or *M. bovis* BCG-infected mice using an RNeasy microkit (Qiagen, Hilden, Germany) following the manufacturer's instructions. For cDNA synthesis, 100 ng of purified total cellular RNA was used. Quantitative real-time reverse transcription-PCR (RT-PCR) was performed on an ABI 7300 real-time PCR system (Applied Biosystems, Warrington, United Kingdom) using SYBR green dye (Eurogentec, Seraing, Belgium). PCR primers for quantification of β-actin (GenBank accession number NM_007393.3), tumor necrosis factor alpha (TNF-α; GenBank accession number M13049), IL-1β (GenBank accession number NM_008361.3), IFN-γ (GenBank accession number NM_008337.3), and inducible nitric oxide (NO) synthase (GenBank accession number NM_010927.3) were designed using Primer Express software (Applied Biosystems, Warrington, United Kingdom), on the basis of the gene sequence data retrieved from GenBank, and were utilized at a concentration of 4 μM. For normalization, β-actin was used as the housekeeping gene, and mean fold changes were calculated using

the $2^{-\Delta\Delta CT}$ threshold cycle (C_T) method (24, 32, 33). All samples were tested in duplicate, and a nontemplate control was included in each amplification run (31).

Quantification of proinflammatory cytokines in spleen homogenates. WT mice and Mincle-KO mice were euthanized, and spleens were collected, homogenized, and then centrifuged at 1,400 rpm and 4°C for 9 min. Cell-free supernatants were collected and stored at −20°C until use. Quantification of proinflammatory cytokines (TNF-α, IFN-γ, IL-1β, RANTES [CCL5]) in cell-free supernatants of spleen homogenates was done using commercially available enzyme-linked immunosorbent assay kits (R&D Systems).

Quantification of NO in spleen homogenates. The release of NO in the spleen tissue of *M. bovis* BCG-infected WT and Mincle-KO mice was analyzed using an NO quantification kit (Active Motif, Rixensart, Belgium), as recently described (31). In brief, spleens were homogenized as outlined above and filtered through a 10-kDa-cutoff micropore filter (Amicon Ultra; Millipore, Billerica, MA, USA). Samples were placed on a 96-well plate, and nitrate reductase and cofactors were added for conversion of nitrate to nitrite. After addition of the Griess reagent, the concentration of NO was determined by using a spectrophotometer operating at an absorbance of 540 nm and a reference wavelength of 620 nm (31).

Statistics. Data are presented as the mean ± standard deviation (SD). Comparisons between groups were performed using Student's *t* test or the Mann-Whitney U test and GraphPad Prism software (version 6.01). Statistically significant differences between treatment groups were assumed when P values were <0.05.

RESULTS

Effect of Mincle deficiency on splenic and hepatic mycobacterial loads and granuloma formation. In a first step, we analyzed whether TDM derived from *M. bovis* is a ligand of Mincle. As shown in Fig. S1 in the supplemental material, Mincle- and FcRγ-expressing NFAT-GFP reporter cells but not FcRγ-only-expressing NFAT-GFP reporter cells responded with a strong GFP fluorescence emission upon exposure to TDM of *M. bovis*, thus verifying that *M. bovis*-derived TDM is a ligand of Mincle.

We next examined the effect of Mincle deficiency on antimycobacterial immunity in the spleens and livers of mice as the main target organs for systemic mycobacterial infections. To mimic a systemic mycobacterial infection, WT mice and Mincle-KO mice were infected intravenously with *M. bovis* BCG. As shown in Fig. 1A, mycobacterial loads were significantly increased in the spleens of Mincle-KO mice relative to those in the spleens of WT mice at days 14, 21, and 28 after intravenous *M. bovis* BCG infection (Fig. 1A), consistent with recent findings (24). Fluorescent auramine and Ziehl-Neelsen (ZN) stainings localized *M. bovis* BCG in the spleen sections, mainly in the white pulp and specifically in clusters of giant cells, of Mincle-KO mice (Fig. 1B). Determination of the number of splenic CFU by classical plating techniques also showed significantly higher mycobacterial loads in the spleens of Mincle-KO mice (Fig. 1C). Increased splenic mycobacterial loads were also observed in WT mice intravenously infected with BCG and subsequently treated with a function-blocking anti-Mincle antibody, 1B6, relative to those observed in the spleens of isotype control Ab-treated BCG-infected WT mice (Fig. 1D). Moreover, Mincle-KO mice responded to intravenous BCG challenge with a significantly reduced splenic granuloma formation compared to that in WT mice (Fig. 1E). Since macrophages represent a major cellular constituent of tuberculous granulomas (4), we also quantified the numbers of macrophages in the splenic granulomas of WT and Mincle-KO mice after intravenous *M. bovis* BCG challenge, using CD68 as a marker for the immunohistochemical enumeration of macrophages in spleen tissue. As shown in Fig. 1F, Mincle-KO mice exhibited a significantly reduced macrophage accumulation in their spleens after i.v. BCG challenge relative to that in the spleens of WT mice.

Similar to our observations in the spleen, we observed that the mycobacterial loads in the livers of Mincle-KO mice were significantly higher than those in the livers of WT mice infected intravenously with *M. bovis* BCG (Fig. 1G). At the same time, no significant differences in granuloma formation were observed in the livers of BCG-challenged WT versus Mincle-KO mice (Fig. 1H), suggesting that, opposed to the spleen, granuloma formation in the liver in response to *M. bovis* BCG infection is not dependent on the presence of Mincle.

Mincle is induced on professional phagocyte subsets in response to intravenous mycobacterial infection in mice. Analysis of the total cell numbers of professional phagocyte subsets in the spleen tissue of mice subjected to i.v. *M. bovis* BCG challenge revealed similar numbers of splenic macrophages in WT and Mincle-KO mice under baseline conditions, with reduced numbers of splenic macrophages being observed in Mincle-KO mice relative to the numbers observed in WT mice on days 14 and 21 postinfection, though the difference did not reach statistical significance (see Fig. S2A in the supplemental material). A significant reduction of the neutrophil counts was observed on day 14 after BCG infection in Mincle-KO mice (see Fig. S2B in the supplemental material). No differences in the numbers of splenic cDCs were noted during the observation period of 21 days (see Fig. S2C in the supplemental material).

Next, we characterized the expression of Mincle on splenic professional phagocytes, including macrophages, neutrophils, dendritic cells, and lymphocytes, of WT mice after intravenous *M. bovis* BCG challenge. Figure 2A to F show the gating strategy employed for analysis of cell surface expression of Mincle on splenic macrophages, neutrophils, and dendritic cells, and Fig. 2G to I show the flow sorting for their subsequent molecular phenotyping by real-time RT-PCR. As shown in Fig. 2J, intravenous infection of mice with *M. bovis* BCG resulted in a delayed, significant induction of Mincle on splenic macrophages that peaked by day 14 postinfection and that showed a decline toward baseline levels by day 21 postinfection. Splenic neutrophils demonstrated a low level of Mincle expression under baseline conditions but showed a timely delayed upregulation of Mincle on their surface after intravenous BCG challenge that peaked by days 7 and 14 postinfection, relative to the Mincle expression of splenic neutrophils of mock-infected WT mice (Fig. 2K). Similar to the findings for splenic macrophages and neutrophils, splenic dendritic cells of WT mice exhibited a low level of Mincle expression under baseline conditions but responded with a marked upregulation of Mincle after i.v. BCG challenge that peaked by day 14 postinfection, with a decline toward the baseline by day 21 postinfection (Fig. 2L). At the same time, splenic lymphocytes lacked Mincle expression in response to i.v. *M. bovis* BCG challenge (data not shown).

Effect of Mincle on proinflammatory gene expression by flow-sorted splenic macrophages, neutrophils, and dendritic cells. Macrophages and neutrophils represent the most important antimycobacterial innate effector cells involved in the uptake and intracellular killing of mycobacterial pathogens (34). Therefore, we next examined the proinflammatory, antimycobacterial gene activation profile of these professional phagocyte subsets in Mincle-KO mice and compared them with those in WT mice after i.v.

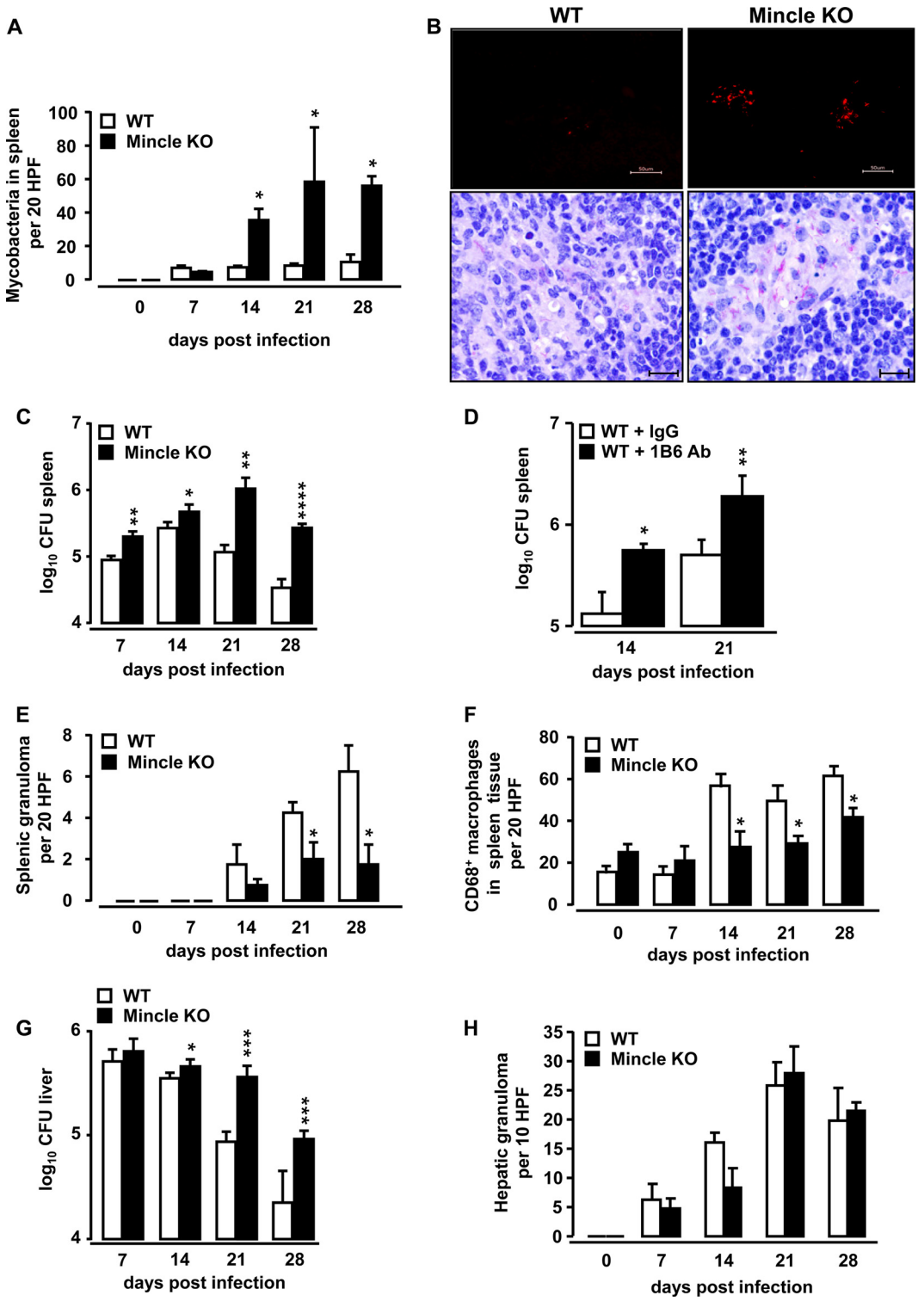

FIG 1 Effect of Mincle deficiency on mycobacterial loads in the spleens and livers of mice infected intravenously with *M. bovis* BCG. WT mice and Mincle-KO mice were infected intravenously with *M. bovis* BCG (8×10^5 CFU/mouse). At the indicated time points, the spleens of mice were analyzed for mycobacterial loads by histopathology and plating techniques (A, C), fluorescent auramine and ZN staining of spleen tissue (B, top and bottom, respectively; 28 days after BCG challenge), as well as determination of granuloma formation (E). The numbers of $CD68^+$ macrophages were determined by immunohistochemical analysis of spleen tissue sections (F). The data are shown as the mean ± SD for 3 mice (0-h time point) or 4 to 5 mice per treatment group and time point *, $P < 0.05$ relative to WT mice; **, $P < 0.001$ relative to WT mice; ****, $P < 0.0001$ relative to WT mice. *P* values were determined by the Mann-Whitney U test (A) or Student's *t* test (C). Bars, 50 μm (B, top) and 20 μm (B, bottom). (D) WT mice were infected intravenously with *M. bovis* BCG (8×10^5 CFU/mouse) and then received daily intraperitoneal injections of either isotype IgG or anti-Mincle Ab 1B6, starting by day 7 postinfection for another 7 or 14 days. Values in panel D are depicted as the mean ± SD for 5 to 7 WT mice treated with isotype IgG and 5 to 9 WT mice treated with anti-Mincle Ab 1B6. The data shown are representative of those from two independently performed experiments. *, $P < 0.05$; **, $P < 0.01$ (Student's *t* test). (G) At the indicated time points, the left and right lateral lobes as well as the caudate lobe of the liver were isolated and subjected to determination of mycobacterial loads by plating techniques. The left and right medial lobes of the liver were subjected to histopathological determination of granuloma formation (enumerated per 10 HPF) (H). Data are shown as the mean ± SD for 3 mice (0-h time point) or 4 or 5 mice per treatment group and time point. *, $P < 0.05$; ***, $P < 0.001$ (Student's *t* test).

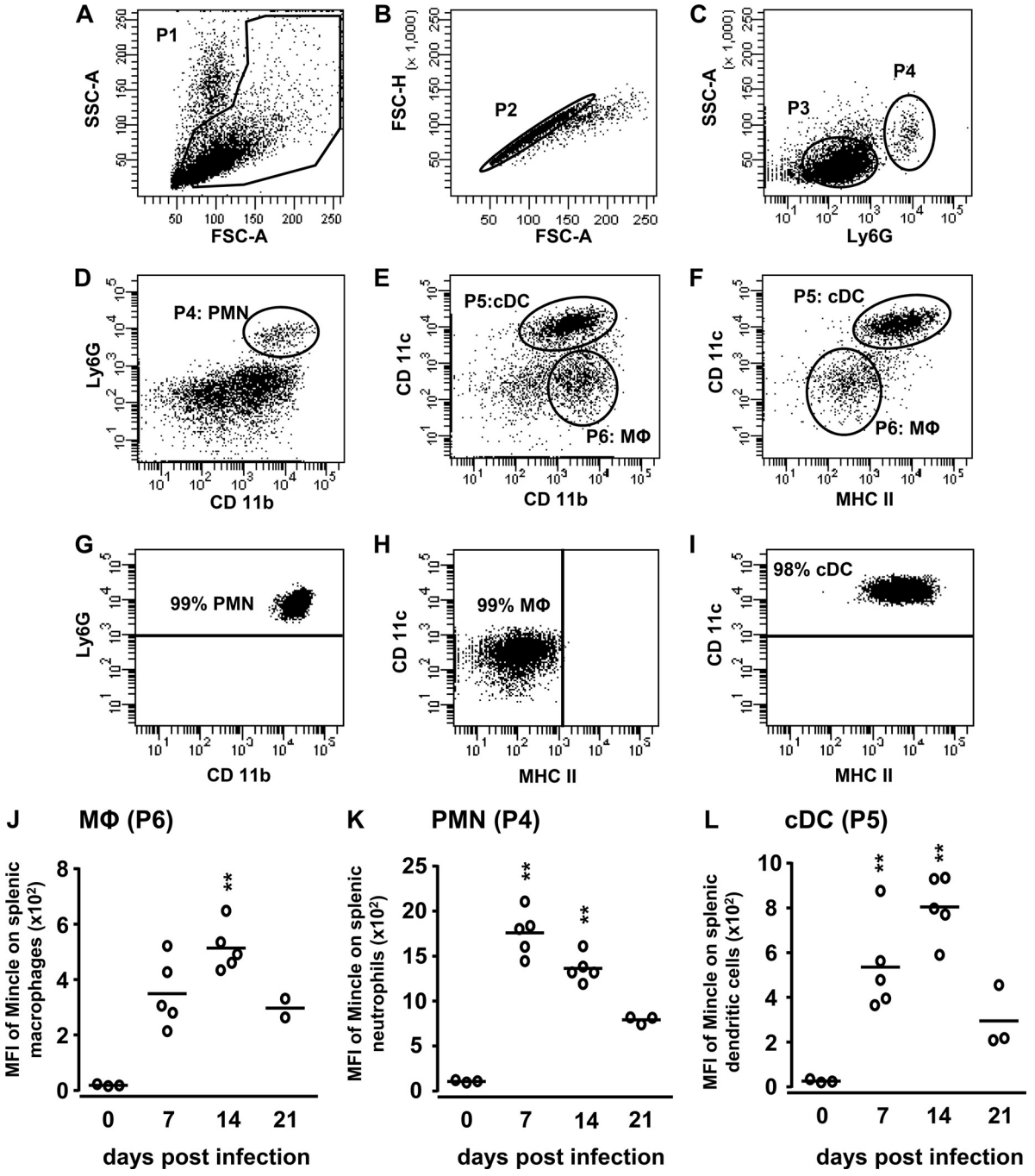

FIG 2 Mincle expression on splenic macrophages, neutrophils, and dendritic cells of mice challenged with *M. bovis* BCG. WT mice were either mock infected (PBS, 0.1% HSA, 0-h values) or infected with *M. bovis* BCG (8×10^5 CFU/mouse). At the indicated time points, the spleens of mice were processed for FACS analysis of Mincle expression on the respective phagocyte populations. Splenic leukocytes were gated according to their FSC-A versus SSC-A characteristics while excluding eosinophils (population 1 [P1]) (for details, see Materials and Methods) (A); this was followed by hierarchical subgating according to their FSC-A versus FSC-H characteristics (P2) (B). After exclusion of $Ly6G^{pos}$, $SSC\text{-}A^{low}$, and $CD11b^{high}$ neutrophils (polymorphonuclear leukocytes [PMNs; P4]) (C, D), $Ly6G^{-}$ leukocytes (P3) (C) were characterized as splenic macrophages (Mϕ; P6) (E, F) according to their $CD11b^{high}$, $CD11c^{low}$, and $MHC\text{-}II^{-/low}$ expression, whereas splenic cDCs were characterized as $CD11c^{high}$, $CD11b^{mid}$, and $MHC\text{-}II^{high}$ (cDCs; P5) (E, F). The purity of flow-sorted splenic neutrophils (polymorphonuclear leukocytes) (G), splenic macrophages (Mϕ) (H), and splenic dendritic cells (cDCs) (I) was determined. At days 0, 7, 14, and 21 after *M. bovis* BCG infection, cell surface expression of Mincle on splenic macrophages (Mϕ; P6) (J), splenic neutrophils (polymorphonuclear leukocytes; P4) (K), and splenic cDCs (cDCs; P5) (L) was analyzed, as indicated. Values are shown as dot plots, with median values indicated as horizontal bars ($n = 3$ to 4 mock-infected mice, $n = 3$ to 6 mice infected with *M. bovis* BCG). **, $P < 0.01$ relative to mock-infected mice (day 0 values) (Mann-Whitney U test).

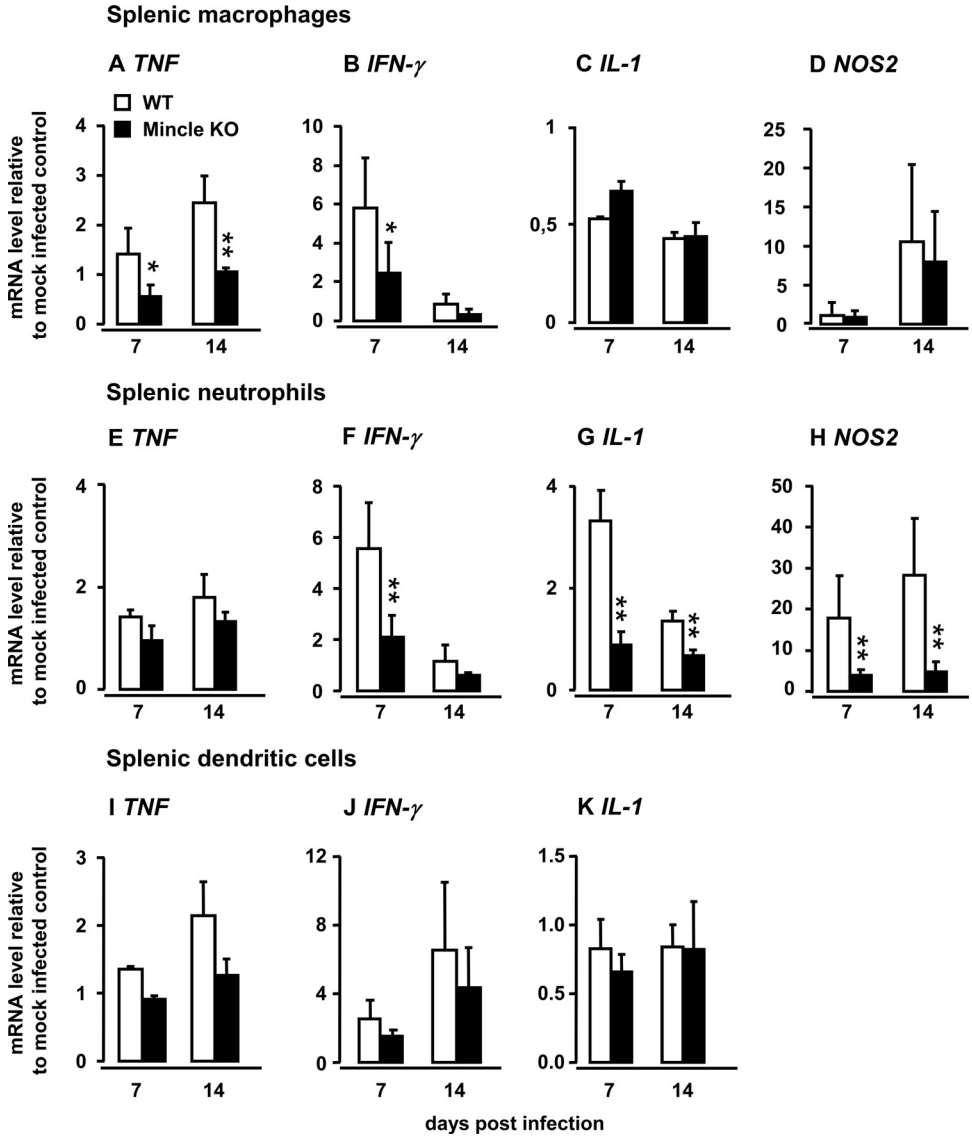

FIG 3 Effect of Mincle deficiency on *M. bovis* BCG-induced gene expression profiles of splenic macrophages, neutrophils, and dendritic cells *in vivo*. WT mice and Mincle-KO mice were either mock infected or infected intravenously with *M. bovis* BCG. Splenic macrophages (A to D) and splenic neutrophils (E to H) were purified by high-speed cell sorting on days 7 and 14 postinfection and subjected to gene expression profiling for TNF (A, E, I), IFN-γ (B, F, J), IL-1 (C, G, K), and NOS2 (D, H) by real-time RT-PCR. Values are shown as the mean ± SD for 3 to 6 mice per time point and experimental group. The data are representative of those from two independently performed experiments. *, $P < 0.05$ relative to WT mice; **, $P < 0.01$ relative to WT mice (Student's *t* test and the Mann-Whitney U test).

BCG challenge. As shown in Fig. 3, splenic macrophages from Mincle-KO mice demonstrated significantly reduced TNF-α and IFN-γ mRNA levels after i.v. BCG challenge relative to those of splenic macrophages collected from WT mice (Fig. 3A and B), whereas no differences between the groups were noted for IL-1 and NOS2 mRNA (Fig. 3C and D). In response to i.v. BCG challenge, splenic neutrophils from Mincle-KO mice responded with IFN-γ mRNA levels and, in particular, IL-1 and NOS2 mRNA levels significantly lower than those of WT neutrophils, whereas no differences in TNF gene expression were noted (Fig. 3E to H). Moreover, in response to intravenous *M. bovis* BCG challenge, flow-sorted splenic cDCs of Mincle-KO mice responded only partially and nonsignificantly with lower levels of TNF and IFN-γ gene expression compared to those of splenic cDCs of WT mice, whereas virtually no differences in IL-1 gene expression were noted between the groups. NOS2 was not detectable in splenic cDCs at days 7 and 14 postinfection, but the opposite was found for NOS2 gene expression by splenic macrophages and neutrophils. These data support the view that Mincle-expressing splenic cDCs are less likely to contribute to the control of splenic mycobacterial loads by the release of proinflammatory Th1 cytokines and illustrate a critical role for Mincle in the regulation of proinflammatory mediator gene induction, especially in splenic macrophages and neutrophils, in response to i.v. challenge of mice with *M. bovis* BCG.

Mincle deficiency limits proinflammatory mediator release in mice after intravenous mycobacterial infection. We next examined the effect of Mincle deficiency on proinflammatory mediator liberation in the spleens of WT and Mincle-KO mice sub-

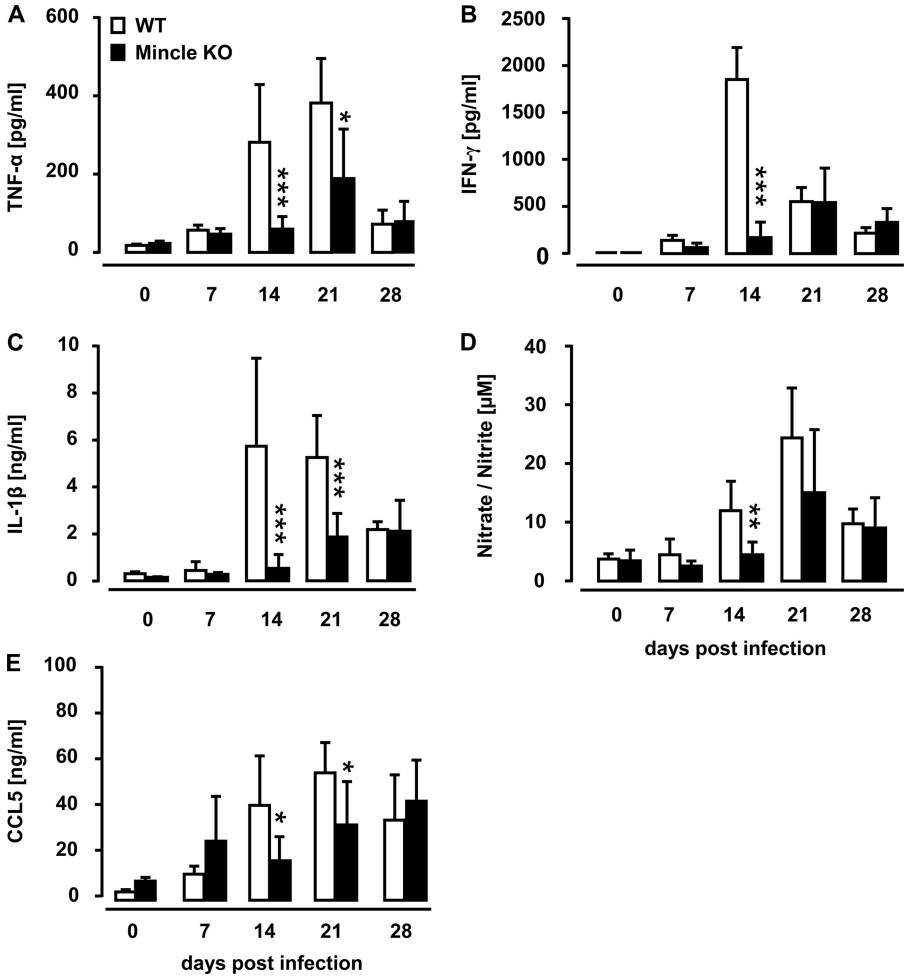

FIG 4 Proinflammatory mediator profiles in spleen homogenates of *M. bovis* BCG-infected WT and Mincle-KO mice. WT mice and Mincle-KO mice were either mock infected (PBS, 0.1% HSA; 0-h values) or infected intravenously with *M. bovis* BCG (8×10^5 CFU/mouse). At the indicated time points, the spleens of infected mice were isolated and homogenized for quantification of TNF-α (A), IFN-γ (B), IL-1β (C), nitric oxide (D), and CCL5 (E). Data are presented as the mean ± SD for 3 mice (0-h time point) and 3 to 7 mice per time point and treatment group. The data are representative of those from two independently performed experiments. *, $P < 0.05$ relative to WT mice; **, $P < 0.01$ relative to WT mice; ***, $P < 0.001$ relative to WT mice (Mann-Whitney U test).

sequent to intravenous *M. bovis* BCG challenge. As shown in Fig. 4A to E, we observed significant differences between WT and Mincle-KO mice in the release of the splenic proinflammatory mediators TNF-α, IFN-γ, IL-1β, CCL5, as well as nitric oxide after i.v. BCG challenge (Fig. 4A to E). These data show that Mincle contributes to the regulation of proinflammatory cytokine and chemokine liberation within the spleens of mice in response to intravenous mycobacterial infection.

Effect of Mincle on accumulation of splenic IFN-γ-producing T cells during systemic mycobacterial infection. T cell-derived IFN-γ is known to be essential for macrophage-dependent antimycobacterial immunity, where it contributes to nitric oxide liberation by activated macrophages (34). Based on our observation that Mincle-KO mice responded with significantly reduced IFN-γ release in their spleens by day 14 after intravenous challenge with *M. bovis* BCG, we next examined the effect of Mincle deficiency on the accumulation of IFN-γ-producing $CD4^+$ and $CD8^+$ T cells in the spleens of mice subjected to intravenous BCG challenge (Fig. 5). We found that Mincle-KO mice responded with a significantly attenuated accumulation of splenic IFN-γ-producing $CD4^+$ and $CD8^+$ T cells by days 7 and 14 after systemic BCG challenge, whereas on days 21 and 28 postinfection, Mincle-KO mice exhibited significantly increased numbers of splenic IFN-γ-producing $CD4^+$ and $CD8^+$ T cells compared to WT mice (Fig. 5A and B). These data show that Mincle is required for the regulation of IFN-γ-producing T cell responses during the early phase of antimycobacterial immunity and a lack of Mincle delays the splenic accumulation of IFN-γ-producing T cells by at least 1 week.

Effect of adoptive WT professional phagocyte transfer on splenic antimycobacterial immunity in Mincle-KO mice. Having shown that the C-type lectin Mincle is expressed on splenic macrophages, neutrophils, and dendritic cells, we next questioned which professional phagocyte subset of Mincle-expressing splenic phagocytes would reverse the attenuated splenic antimycobacterial immunity in Mincle-KO mice. Mincle-KO mice received a single adoptive transfer of bone marrow-derived monocytes from WT mice or Mincle-KO mice (which served as transfusion controls) subsequent to i.v. infection with BCG. As shown in Fig. 6A, adoptive transfer of WT but not Mincle-KO bone marrow-de-

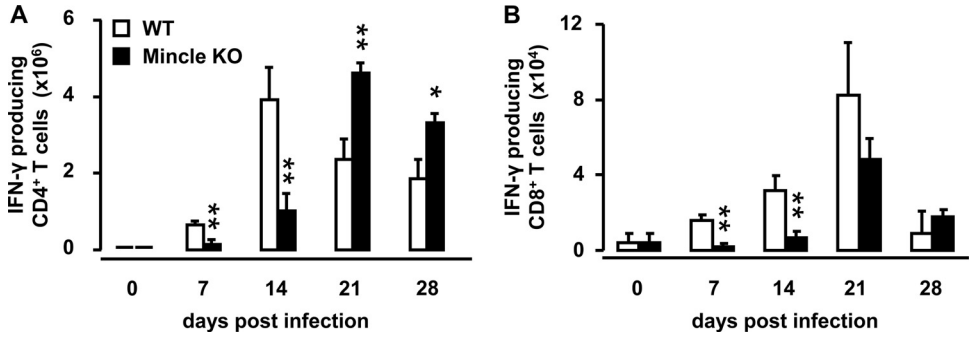

FIG 5 Effect of Mincle deficiency on numbers of splenic IFN-γ-producing T cell subsets in mice infected with *M. bovis* BCG. WT mice and Mincle-KO mice were either mock infected (0-h values) or infected intravenously with *M. bovis* BCG (8×10^5 CFU/mouse). At the indicated time points postinfection, the numbers of IFN-γ-producing splenic $CD4^+$ and $CD8^+$ T cells were quantified by flow cytometry. Data are shown as the mean ± SD for 3 to 10 mice per time point and treatment group. *, $P < 0.05$ relative to WT mice; **, $P < 0.01$ relative to WT mice (Mann-Whitney U test).

rived monocytes into Mincle-KO mice resulted in significantly reduced splenic mycobacterial loads on days 14 and 21 postinfection (Fig. 6A), together with significantly increased numbers of IFN-γ-producing $CD4^+$ and $CD8^+$ T cells and increased levels of the lymphocyte chemoattractant CCL5 in the spleens of recipient Mincle-KO mice on day 14 after intravenous BCG challenge (Fig. 6B to D).

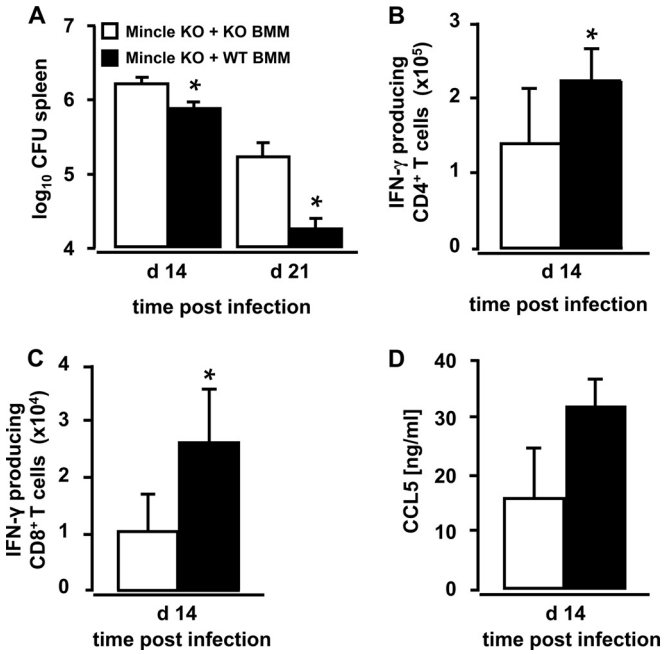

FIG 6 Effect of adoptive transfer of BMMs on antimycobacterial immunity in Mincle-KO mice. BMMs (5×10^6 cells/mouse) from WT or Mincle-KO mice were transfused into Mincle-KO mice immediately subsequent to intravenous infection with *M. bovis* BCG. (A) At 14 and 21 days postinfection, the mycobacterial loads in the spleens of Mincle-KO mice transfused with WT or Mincle-KO BMMs were determined. d, day. (B, C) Numbers of IFN-γ-producing $CD4^+$ (B) and $CD8^+$ (C) T cells in splenic tissue digests of Mincle-KO mice transfused with WT or Mincle-KO BMMs. (D) CCL5 levels in cell-free supernatants of spleen homogenates from i.v. *M. bovis* BCG-infected Mincle-KO mice after adoptive transfer of WT or Mincle-KO BMMs. The data are shown as the mean ± SD for 4 to 11 mice per time point and treatment group. Data are representative of those from three independently performed experiments. *, $P < 0.05$ relative to Mincle-KO mice receiving Mincle-KO monocytes by Student's *t* test (A) and the Mann-Whitney U test (B to D).

Adoptive transfer of bone marrow-derived monocytes from WT mice into Mincle-KO mice may give rise to splenic macrophages and/or cDCs, both of which may contribute to the improved antimycobacterial immunity in adoptively transfused Mincle-KO mice shown in Fig. 6. Therefore, we established a protocol to selectively deplete monocyte-derived cDCs, while sparing monocyte-derived macrophages, to allow analysis of the relative impact of donor-derived DCs as opposed to macrophages on splenic antimycobacterial immunity in adoptively transfused Mincle-KO mice (Fig. 7). To accomplish this, we transfused bone marrow-derived monocytes from transgenic $zDC^{+/DTR}$ mice into BCG-infected CD45.1 recipient mice. Such adoptively transfused CD45.1 mice were then i.p. treated with DT every 48 h for 7 days to deplete monocyte-derived cDCs, which are known to specifically express the DT receptor under the control of the transcription factor zDC, while at the same time spare monocytes and macrophages (or other leukocytes) derived from monocytes lacking transgenic DTR expression (25). As shown in Fig. 7A to E, transfusion of $CD45.2^+$ donor monocytes from transgenic $zDC^{+/DTR}$ mice into BCG-challenged CD45.1 recipient mice resulted in the splenic accumulation of CD45.2 donor leukocytes consisting of equal amounts of both $CD11c^{high}$ and MHC-II^{high} donor DCs and $CD11c^{low}$ and MHC-II^- splenic donor macrophages (Fig. 7D, E, and H). Subsequent treatment of $CD45.1^+$ recipient mice adoptively transfused with bone marrow-derived monocytes from $CD45.2^+$ $zDC^{+/DTR}$ mice with DT selectively depleted $CD45.2^+$ $zDC^{+/DTR}$ splenic donor-type DCs while at the same time spared donor-type $CD45.2^+$ splenic macrophages (Fig. 7F, G, and I).

We then elucidated the relative contribution of donor-derived DCs versus macrophages to improve splenic antimycobacterial immunity in Mincle-KO mice. Mincle-KO mice adoptively transfused with bone marrow-derived monocytes from $zDC^{+/DTR}$ mice subsequent to BCG challenge responded to DT treatment with both significantly increased splenic mycobacterial loads and, at the same time, significantly reduced amounts of IFN-γ-producing $CD4^+$ T cells relative to the results for adoptively transfused, PBS-treated Mincle-KO mice (Fig. 7J and K).

In contrast, even repetitive adoptive transfer of WT neutrophils into recipient Mincle-KO mice performed on days 0, 3, and 5 after intravenous BCG challenge did not show any effect on either the mycobacterial loads in the spleens of recipient Mincle-KO mice (see Fig. S3A in the supplemental material) or the numbers of IFN-γ-producing $CD4^+$ and $CD8^+$ T cells (see

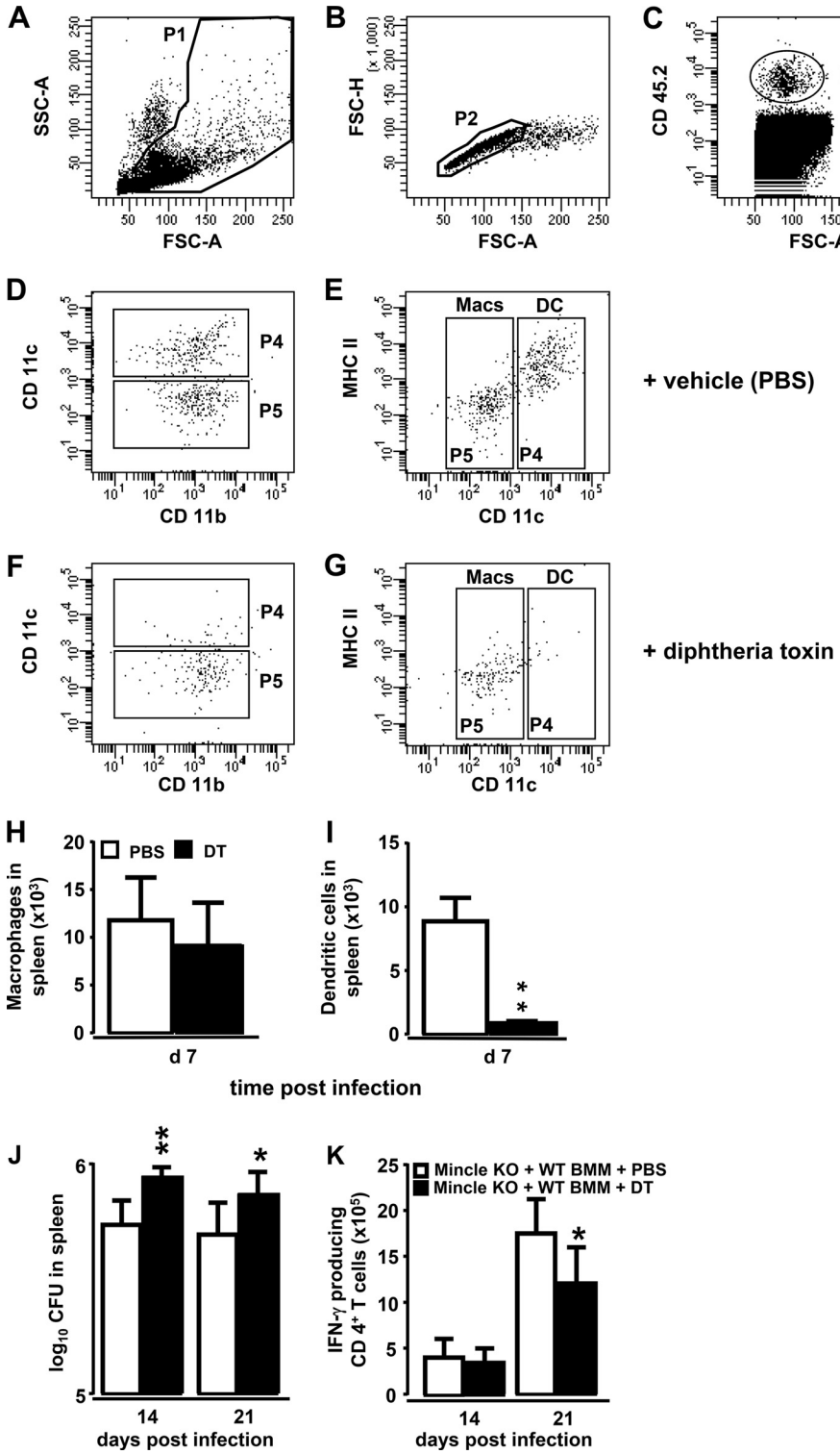

FIG 7 DT-induced depletion of donor-type dendritic cells in spleens of recipient mice. BMMs from CD45.2$^+$ zDC$^{+/DTR}$ mice (5×10^6 cells/mouse) were adoptively transferred into CD45.1$^+$ recipient mice subsequent to their intravenous infection with *M. bovis* BCG. Seven days after adoptive transfer, splenocytes were processed and gated according to their FSC-A/SSC-A characteristics (population 1 [P1]) (A) and FSC-A/FSC-H characteristics (P2) (B), followed by gating of the CD45.2$^+$ donor-type leukocytes (P3) (C). (D, E) Hierarchical subgating of P3 revealed two major populations, P4 and P5, according to their differential CD11c and MHC-II expression, and these were further characterized as splenic cDCs (P4), according to their CD11c^{high} and MHC-II^{high} antigen expression, and splenic macrophages, according to their CD11c^{low} and MHC-II^{low} antigen expression (P5). Treatment of adoptively transfused mice with DT (10 ng/g bw in PBS) (F, G) but not vehicle (PBS only) (D, E) led to a selective and significant depletion of splenic CD45.2$^+$ cDCs but not macrophages (P4) (F, G, H, I), thus functionally confirming that cells of P4 are donor-type CD45.2$^+$/zDC$^{+/DTR}$ splenic cDCs. The data in panels H and I are shown as the mean ± SD for 5 mice per treatment group. **, $P < 0.01$ relative to PBS treatment (Mann-Whitney U test). (J, K) Mincle-KO mice were infected intravenously with *M. bovis* BCG (8×10^5 CFU/mouse), followed by adoptive transfer of bone marrow-derived monocytes (5×10^6 cells/mouse) from transgenic zDC$^{+/DTR}$ donor mice. Subsequently, the mice were treated i.p. with either PBS or DT. On days 14 and 21 postinfection, the numbers of splenic mycobacterial CFU (J) or the numbers of IFN-γ-producing CD4$^+$ T cells (K) were determined. The data are presented as the mean ± SD for 5 to 14 mice per time point and treatment group. **, $P < 0.01$ relative to PBS treatment; *, $P < 0.05$, relative to PBS treatment (Student's *t* test).

Fig. S3B and C in the supplemental material) relative to the results for BCG-infected Mincle-KO mice repetitively transfused with neutrophils from donor Mincle-KO mice.

Finally, we examined what effect the transfusion of Mincle-KO mice with Mincle-expressing WT donor mononuclear phagocyte subsets either depleted or not depleted of cDCs would have on liver mycobacterial loads. As opposed to the spleen, where diphtheria toxin-dependent cDC depletion led to significantly increased numbers of splenic CFU, no such effect was observed in the liver (see Fig. S4A in the supplemental material). In addition, we did not find any effect of WT monocyte/macrophage transfusion (in the absence or presence of diphtheria toxin) on IFN-γ-producing T cell subsets in the livers of i.v. *M. bovis* BCG-infected Mincle-KO mice (see Fig. S4B and C in the supplemental material).

DISCUSSION

The current study was designed to elucidate the role of Mincle in the control of systemic mycobacterial infection in mice challenged intravenously with *M. bovis* BCG. Mincle-deficient mice exhibited strongly increased mycobacterial loads in their spleen and liver, while granuloma formation was attenuated only in the spleen and not the liver of BCG-challenged Mincle-KO mice. The impaired splenic antimycobacterial response of Mincle-KO mice observed was accompanied by strongly attenuated Th1 cytokine release and, in particular, diminished accumulation of IFN-γ-producing T cell subsets in the spleens of mutant mice. Importantly, adoptive transfer experiments revealed a contribution of Mincle-expressing cDCs to the regulation of splenic but not hepatic antimycobacterial immunity in mice.

In a recent report, we characterized an important role for Mincle in regulating lung protective immunity against pulmonary *M. bovis* BCG infection in mice (24). At the same time, we observed that Mincle-KO mice were more susceptible to intravenous mycobacterial infection than WT mice, suggesting that the C-type lectin Mincle might also regulate extrapulmonary antimycobacterial responses. However, the role of Mincle in the regulation of antimycobacterial immunity during systemic mycobacterial infections in spleen and liver, as well as the underlying Mincle-expressing effector cell type(s), has not been determined so far. We used an intravenous route of mycobacterial infection as an experimental model for systemic mycobacterial infection. We found significantly higher mycobacterial loads in both the spleen and the liver of *M. bovis* BCG-infected Mincle-KO mice than in the spleen and liver of *M. bovis* BCG-infected WT mice. At the same time, granuloma formation was attenuated only in the spleen and not in the liver of mutant mice, suggesting that Mincle is not required for hepatic granuloma formation. Moreover, Mincle-KO mice demonstrated significantly increased hepatic mycobacterial loads after systemic BCG challenge compared to those in WT mice during an observation period of 28 days. At the same time, adoptive WT cell transfusion experiments in Mincle-KO mice had no effect on hepatic mycobacterial loads, which is just the opposite result found for the spleen. These data suggest a differential, organ-specific contribution of Mincle to granuloma formation and antimycobacterial immunity, which is found in lymphoid organs (spleen) but not nonlymphoid organs (liver) of mice. Future studies are needed to examine what Mincle-independent mechanisms possibly mediated by other (C-type lectin) pattern recognition receptors mediate granuloma formation in the liver of mice.

We found that adoptively transfused bone marrow-derived monocytes from $zDC^{+/DTR}$ mice maintained their full plasticity to differentiate to a similar extent into both Mincle-expressing DCs and Mincle-expressing macrophages in the spleens of BCG-challenged Mincle-KO mice. Considering that the transcription factor zDC (also termed Zbtb46) is specifically expressed by conventional DCs but not macrophages (25), the currently employed diphtheria toxin-induced DC depletion protocol for the first time allows dissection of the respective contributions of Mincle-expressing splenic cDCs versus those of Mincle-expressing macrophages to antimycobacterial immune responses in a Mincle-deficient background. Our data show (i) that Mincle-expressing splenic DCs contribute to splenic but not hepatic antimycobacterial immunity and (ii) that the observed effect of Mincle-expressing cDCs on mycobacterial loads and the numbers of IFN-γ-producing T cell subsets cannot be fully compensated for by Mincle-expressing splenic macrophages in the absence of Mincle-expressing splenic cDCs. Given that splenic T cells were not observed to express Mincle (data not shown) and, further, given that Mincle expression on splenic DCs was necessary to elicit increased numbers of splenic IFN-γ-producing $CD4^+$ and $CD8^+$ T cells in a Mincle-deficient background, Mincle likely primes cDCs directly to respond as antigen-presenting cells (APCs) to mycobacterial pathogen-associated molecular patterns (PAMPs), such as TDM, to provide T cell-stimulatory signals in mycobacterium-infected mice. However, this concept warrants future examination.

The fact that Mincle-expressing neutrophils were not able to reverse the observed splenic phenotype in BCG-challenged Mincle-KO mice might have been due to the fact that neutrophils, unlike macrophages, are short-lived leukocyte subsets which do not act as antigen-presenting cells to enhance acquired immune responses to mycobacterial challenge but, rather, have been shown to enhance lung inflammation in response to TDM (35). As such, transfusion of Mincle-expressing donor neutrophils into recipient Mincle-KO mice did not trigger increased accumulation of IFN-γ-producing T cell subsets in the spleens of mice. To address the issue of the short half-life of transfused neutrophils that may have confounded the experimental results, BCG-challenged Mincle-KO mice received repetitive intravenous transfusions of WT neutrophils on days 0, 3, and 5 after i.v. BCG challenge to allow us to largely rule out the possibility that just an insufficient availability of splenic WT neutrophils was responsible for the observed lack of neutrophil transfusion efficacy in terms of IFN-γ-producing T cell responses in the Mincle-KO mice.

We observed here that Mincle-KO mice, known to signal via the Syk/Card9 adaptor pathway, demonstrated significantly increased mycobacterial loads along with decreased numbers of IFN-γ-producing T cell subsets in their spleens subsequent to systemic BCG challenge. Similarly, $Card9^{-/-}$ mice have also previously been shown to respond with significantly increased mycobacterial loads in their lungs upon challenge with *M. tuberculosis* (36). At the same time, however, other reports demonstrated that $Card9^{-/-}$ mice exhibited significantly increased numbers of IFN-γ-producing T cells in lung draining lymph nodes relative to the numbers in *M. tuberculosis*-infected WT mice, resulting in rapid mortality after *M. tuberculosis* infection (23). This finding is quite opposite what we observed in Mincle-KO mice exhibiting decreased numbers of IFN-γ-producing T cells after BCG challenge. Generally, it is well established that adaptor molecules, such as

Card9 sampling signals from various pattern recognition receptor, including C-type lectin receptors, RIG-1-like helicases, NOD-like receptors, and Toll-like receptors, are more essential for survival after mycobacterial challenge than deletion of single receptor checkpoints (36). Several reasons may explain the differences in the T cell responses observed in mycobacterium-infected Mincle-KO mice and Card9-KO mice, including the use of different organ systems (spleen versus lung and lung draining lymph nodes), differences in the route of mycobacterial infection (the intratracheal versus i.v. infection route), as well as differences in the pathogenicity profiles between *M. bovis* BCG and *M. tuberculosis*.

The role of Mincle in protective antimycobacterial immunity is still controversial. Heitmann et al. (37) reported no essential impact of the C-type lectin Mincle on protective immunity against *M. tuberculosis*. In contrast, Lee et al. reported a role for Mincle in TDM-induced neutrophil activation and liberation of proinflammatory mediators, overall showing increased lung mycobacterial loads and immune pathology in Mincle-KO mice infected with *M. tuberculosis* Erdmann (38). Moreover, infection of bone marrow-derived macrophages from WT and Mincle-KO mice infected with *M. bovis* BCG *in vitro* revealed reduced NO production and granulocyte colony-stimulating factor secretion in Mincle-deficient bone marrow-derived macrophages (37), and the current study and our recently published data (24) also support a role for Mincle in antimycobacterial immunity against *M. bovis* BCG. Differences in the virulence profiles of the employed mycobacterial strains (*M. tuberculosis* H37Rv, *M. tuberculosis* Erdman, and *M. bovis* BCG) and differences in mycobacterial administration routes may explain, at least in part, the reported differences between the studies.

The attenuated antimycobacterial response of Mincle-KO mice to intravenous BCG challenge was recapitulated to a large extent in i.v. BCG-infected WT mice treated with the function-blocking anti-Mincle antibody 1B6, with the treatment overall resulting in significantly increased mycobacterial loads in the spleens of mice during an observation period of 21 days. In this regard, Miyake et al. (39) most recently demonstrated a weak cross-reactivity of the currently employed anti-Mincle antibody 1B6 with the newly characterized C-type lectin macrophage C-type lectin (MCL; also called Clec4d). MCL is likely to arise from duplication of the gene for Mincle, is constitutively expressed on macrophages, and, like Mincle, is also an activating receptor that mediates the adjuvanticity of TDM (24, 39). Our recently published data from a study employing antibody 1B6 to monitor Mincle expression on alveolar macrophages in response to various mycobacterial PAMPs *in vitro* demonstrated only a very weak immunoreactivity of 1B6 with Mincle-KO macrophages, which constitutively express MCL, thus supporting the view that 1B6 has a very weak affinity of binding to MCL, as opposed to its high affinity of binding to Mincle (24, 39). Therefore, we believe that the *in vivo* blockade observed in the currently reported experiments employing antibody 1B6 were, for the most part, due to a specific Mincle blockade by 1B6, rather than a low-level cross-reactivity of antibody 1B6 with the C-type lectin MCL.

In conclusion, we show that the C-type lectin Mincle is an important pattern recognition receptor that contributes to the control of splenic and hepatic mycobacterial infections after systemic *M. bovis* BCG infection in mice. These data may be an important basis for future preclinical studies to modulate Mincle expression *in vivo* with the aim of accelerating the Mincle-dependent onset of antimycobacterial responses and, thus, host protective immunity against mycobacterial challenge.

ACKNOWLEDGMENTS

We thank Regina Engelhardt for her excellent technical support.

Each us declares no conflict of interest.

This work was supported by the Society of Lower Saxony for the Control of Tuberculosis, the Hannover Biomedical Research School (HBRS), and the Center for Infection Biology (ZIB) of Hannover Medical School.

REFERENCES

1. **WHO.** 2012. Global tuberculosis report 2012. WHO, Geneva, Switzerland.
2. **Kaufmann SH.** 2001. How can immunology contribute to the control of tuberculosis? Nat Rev Immunol **1:**20–30. http://dx.doi.org/10.1038/35095558.
3. **Ernst JD.** 2012. The immunological life cycle of tuberculosis. Nat Rev Immunol **12:**581–591. http://dx.doi.org/10.1038/nri3259.
4. **Ramakrishnan L.** 2012. Revisiting the role of the granuloma in tuberculosis. Nat Rev Immunol **12:**352–366. http://dx.doi.org/10.1038/nri3211.
5. **Gengenbacher M, Kaufmann SH.** 2012. Mycobacterium tuberculosis: success through dormancy. FEMS Microbiol Rev **36:**514–532. http://dx.doi.org/10.1111/j.1574-6976.2012.00331.x.
6. **Flynn JL, Chan J, Lin PL.** 2011. Macrophages and control of granulomatous inflammation in tuberculosis. Mucosal Immunol **4:**271–278. http://dx.doi.org/10.1038/mi.2011.14.
7. **Steinwede K, Maus R, Bohling J, Voedisch S, Braun A, Ochs M, Schmiedl A, Langer F, Gauthier F, Roes J, Welte T, Bange FC, Niederweis M, Buhling F, Maus UA.** 2012. Cathepsin G and neutrophil elastase contribute to lung-protective immunity against mycobacterial infections in mice. J Immunol **188:**4476–4487. http://dx.doi.org/10.4049/jimmunol.1103346.
8. **Guirado E, Schlesinger LS.** 2013. Modeling the Mycobacterium tuberculosis granuloma—the critical battlefield in host immunity and disease. Front Immunol **4:**98. http://dx.doi.org/10.3389/fimmu.2013.00098.
9. **Ehlers S, Schaible UE.** 2012. The granuloma in tuberculosis: dynamics of a host-pathogen collusion. Front Immunol **3:**411. http://dx.doi.org/10.3389/fimmu.2012.00411.
10. **Marakalala MJ, Graham LM, Brown GD.** 2010. The role of Syk/CARD9-coupled C-type lectin receptors in immunity to Mycobacterium tuberculosis infections. Clin Dev Immunol **2010:**567571. http://dx.doi.org/10.1155/2010/567571.
11. **Sharma SK, Mohan A, Sharma A, Mitra DK.** 2005. Miliary tuberculosis: new insights into an old disease. Lancet Infect Dis **5:**415–430. http://dx.doi.org/10.1016/S1473-3099(05)70163-8.
12. **Krishnan N, Robertson BD, Thwaites G.** 2010. The mechanisms and consequences of the extra-pulmonary dissemination of Mycobacterium tuberculosis. Tuberculosis (Edinb) **90:**361–366. http://dx.doi.org/10.1016/j.tube.2010.08.005.
13. **Ray S, Talukdar A, Kundu S, Khanra D, Sonthalia N.** 2013. Diagnosis and management of miliary tuberculosis: current state and future perspectives. Ther Clin Risk Manag **9:**9–26. http://dx.doi.org/10.2147/TCRM.S29179.
14. **Steg A, Sicard D, Leleu C, Debre B, Boccon-Gibod L.** 1985. Systemic complications of intravesical BCG therapy for bladder cancer. Lancet **ii:**899.
15. **Matsumoto M, Tanaka T, Kaisho T, Sanjo H, Copeland NG, Gilbert DJ, Jenkins NA, Akira S.** 1999. A novel LPS-inducible C-type lectin is a transcriptional target of NF-IL6 in macrophages. J Immunol **163:**5039–5048.
16. **Flornes LM, Bryceson YT, Spurkland A, Lorentzen JC, Dissen E, Fossum S.** 2004. Identification of lectin-like receptors expressed by antigen presenting cells and neutrophils and their mapping to a novel gene complex. Immunogenetics **56:**506–517. http://dx.doi.org/10.1007/s00251-004-0714-x.
17. **Yamasaki S, Ishikawa E, Sakuma M, Hara H, Ogata K, Saito T.** 2008. Mincle is an ITAM-coupled activating receptor that senses damaged cells. Nat Immunol **9:**1179–1188. http://dx.doi.org/10.1038/ni.1651.
18. **Ishikawa E, Ishikawa T, Morita YS, Toyonaga K, Yamada H, Takeuchi O, Kinoshita T, Akira S, Yoshikai Y, Yamasaki S.** 2009. Direct recognition of

the mycobacterial glycolipid, trehalose dimycolate, by C-type lectin Mincle. J Exp Med **206:**2879–2888. http://dx.doi.org/10.1084/jem.20091750.
19. **Schoenen H, Bodendorfer B, Hitchens K, Manzanero S, Werninghaus K, Nimmerjahn F, Agger EM, Stenger S, Andersen P, Ruland J, Brown GD, Wells C, Lang R.** 2010. Cutting edge: Mincle is essential for recognition and adjuvanticity of the mycobacterial cord factor and its synthetic analog trehalose-dibehenate. J Immunol **184:**2756–2760. http://dx.doi.org/10.4049/jimmunol.0904013.
20. **Yamasaki S, Matsumoto M, Takeuchi O, Matsuzawa T, Ishikawa E, Sakuma M, Tateno H, Uno J, Hirabayashi J, Mikami Y, Takeda K, Akira S, Saito T.** 2009. C-type lectin Mincle is an activating receptor for pathogenic fungus, Malassezia. Proc Natl Acad Sci U S A **106:**1897–1902. http://dx.doi.org/10.1073/pnas.0805177106.
21. **Wells CA, Salvage-Jones JA, Li X, Hitchens K, Butcher S, Murray RZ, Beckhouse AG, Lo YL, Manzanero S, Cobbold C, Schroder K, Ma B, Orr S, Stewart L, Lebus D, Sobieszczuk P, Hume DA, Stow J, Blanchard H, Ashman RB.** 2008. The macrophage-inducible C-type lectin, Mincle, is an essential component of the innate immune response to Candida albicans. J Immunol **180:**7404–7413. http://dx.doi.org/10.4049/jimmunol.180.11.7404.
22. **Ishikawa T, Itoh F, Yoshida S, Saijo S, Matsuzawa T, Gonoi T, Saito T, Okawa Y, Shibata N, Miyamoto T, Yamasaki S.** 2013. Identification of distinct ligands for the C-type lectin receptors Mincle and Dectin-2 in the pathogenic fungus Malassezia. Cell Host Microbe **13:**477–488. http://dx.doi.org/10.1016/j.chom.2013.03.008.
23. **Werninghaus K, Babiak A, Gross O, Holscher C, Dietrich H, Agger EM, Mages J, Mocsai A, Schoenen H, Finger K, Nimmerjahn F, Brown GD, Kirschning C, Heit A, Andersen P, Wagner H, Ruland J, Lang R.** 2009. Adjuvanticity of a synthetic cord factor analogue for subunit Mycobacterium tuberculosis vaccination requires FcRgamma-Syk-Card9-dependent innate immune activation. J Exp Med **206:**89–97. http://dx.doi.org/10.1084/jem.20081445.
24. **Behler F, Steinwede K, Balboa L, Ueberberg B, Maus R, Kirchhof G, Yamasaki S, Welte T, Maus UA.** 2012. Role of Mincle in alveolar macrophage-dependent innate immunity against mycobacterial infections in mice. J Immunol **189:**3121–3129. http://dx.doi.org/10.4049/jimmunol.1201399.
25. **Meredith MM, Liu K, Darrasse-Jeze G, Kamphorst AO, Schreiber HA, Guermonprez P, Idoyaga J, Cheong C, Yao KH, Niec RE, Nussenzweig MC.** 2012. Expression of the zinc finger transcription factor zDC (Zbtb46, Btbd4) defines the classical dendritic cell lineage. J Exp Med **209:**1153–1165. http://dx.doi.org/10.1084/jem.20112675.
26. **Steinwede K, Henken S, Bohling J, Maus R, Ueberberg B, Brumshagen C, Brincks EL, Griffith TS, Welte T, Maus UA.** 2012. TNF-related apoptosis-inducing ligand (TRAIL) exerts therapeutic efficacy for the treatment of pneumococcal pneumonia in mice. J Exp Med **209:**1937–1952. http://dx.doi.org/10.1084/jem.20120983.
27. **Taut K, Winter C, Briles DE, Paton JC, Christman JW, Maus R, Baumann R, Welte T, Maus UA.** 2008. Macrophage turnover kinetics in the lungs of mice infected with Streptococcus pneumoniae. Am J Respir Cell Mol Biol **38:**105–113. http://dx.doi.org/10.1165/rcmb.2007-0132OC.
28. **Maus UA, Waelsch K, Kuziel WA, Delbeck T, Mack M, Blackwell TS, Christman JW, Schlondorff D, Seeger W, Lohmeyer J.** 2003. Monocytes are potent facilitators of alveolar neutrophil emigration during lung inflammation: role of the CCL2-CCR2 axis. J Immunol **170:**3273–3278. http://dx.doi.org/10.4049/jimmunol.170.6.3273.
29. **Hahn I, Klaus A, Janze AK, Steinwede K, Ding N, Bohling J, Brumshagen C, Serrano H, Gauthier F, Paton JC, Welte T, Maus UA.** 2011. Cathepsin G and neutrophil elastase play critical and nonredundant roles in lung-protective immunity against Streptococcus pneumoniae in mice. Infect Immun **79:**4893–4901. http://dx.doi.org/10.1128/IAI.05593-11.
30. **Rose S, Misharin A, Perlman H.** 2012. A novel Ly6C/Ly6G-based strategy to analyze the mouse splenic myeloid compartment. Cytometry A **81:**343–350. http://dx.doi.org/10.1002/cyto.a.22012.
31. **Brumshagen C, Maus R, Bischof A, Ueberberg B, Bohling J, Osterholzer JJ, Ogunniyi AD, Paton JC, Welte T, Maus UA.** 2012. FMS-like tyrosine kinase 3 ligand treatment of mice aggravates acute lung injury in response to Streptococcus pneumoniae: role of pneumolysin. Infect Immun **80:**4281–4290. http://dx.doi.org/10.1128/IAI.00854-12.
32. **Srivastava M, Meinders A, Steinwede K, Maus R, Lucke N, Buhling F, Ehlers S, Welte T, Maus UA.** 2007. Mediator responses of alveolar macrophages and kinetics of mononuclear phagocyte subset recruitment during acute primary and secondary mycobacterial infections in the lungs of mice. Cell Microbiol **9:**738–752. http://dx.doi.org/10.1111/j.1462-5822.2006.00824.x.
33. **Livak KJ, Schmittgen TD.** 2001. Analysis of relative gene expression data using real-time quantitative PCR and the 2(−delta delta C(T)) method. Methods **25:**402–408. http://dx.doi.org/10.1006/meth.2001.1262.
34. **O'Garra A, Redford PS, McNab FW, Bloom CI, Wilkinson RJ, Berry MP.** 2013. The immune response in tuberculosis. Annu Rev Immunol **31:**475–527. http://dx.doi.org/10.1146/annurev-immunol-032712-095939.
35. **Kolaczkowska E, Kubes P.** 2013. Neutrophil recruitment and function in health and inflammation. Nat Rev Immunol **13:**159–175. http://dx.doi.org/10.1038/nri3399.
36. **Dorhoi A, Desel C, Yeremeev V, Pradl L, Brinkmann V, Mollenkopf HJ, Hanke K, Gross O, Ruland J, Kaufmann SH.** 2010. The adaptor molecule CARD9 is essential for tuberculosis control. J Exp Med **207:**777–792. http://dx.doi.org/10.1084/jem.20090067.
37. **Heitmann L, Schoenen H, Ehlers S, Lang R, Holscher C.** 2013. Mincle is not essential for controlling Mycobacterium tuberculosis infection. Immunobiology **218:**506–516. http://dx.doi.org/10.1016/j.imbio.2012.06.005.
38. **Lee WB, Kang JS, Yan JJ, Lee MS, Jeon BY, Cho SN, Kim YJ.** 2012. Neutrophils promote mycobacterial trehalose dimycolate-induced lung inflammation via the Mincle pathway. PLoS Pathog **8:**e1002614. http://dx.doi.org/10.1371/journal.ppat.1002614.
39. **Miyake Y, Toyonaga K, Mori D, Kakuta S, Hoshino Y, Oyamada A, Yamada H, Ono K, Suyama M, Iwakura Y, Yoshikai Y, Yamasaki S.** 2013. C-type lectin MCL is an FcRgamma-coupled receptor that mediates the adjuvanticity of mycobacterial cord factor. Immunity **38:**1050–1062. http://dx.doi.org/10.1016/j.immuni.2013.03.010.